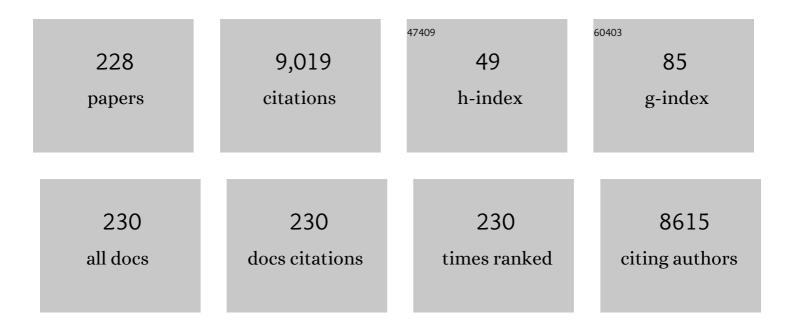
Xian-Ming Zhang

List of Publications by Year in descending order

Source: https://exaly.com/author-pdf/6611080/publications.pdf Version: 2024-02-01



#	Article	IF	CITATIONS
1	<scp>Singleâ€Molecule</scp> Confinement Induced Intrinsic <scp>Multiâ€Electron Redoxâ€Activity</scp> to Enhance Supercapacitor Performance. Energy and Environmental Materials, 2023, 6, .	7.3	5
2	Synergistic effect of Nill and Co/FellI in doped mixed-valence phosphonate for enhancing electrocatalytic oxygen evolution. Green Energy and Environment, 2022, 7, 432-439.	4.7	8
3	A Photoâ€Responsive Chargeâ€Assisted Hydrogenâ€Bonded Organic Network with Ultraâ€6table Viologen Radicals. Chinese Journal of Chemistry, 2022, 40, 351-356.	2.6	14
4	Ca-cluster-constructed deep-ultraviolet nonlinear-optical crystal Na2Ca17Al2(PO4)14 with strong NLO response. Journal of Alloys and Compounds, 2022, 896, 162975.	2.8	2
5	Lead Tellurite Crystals BaPbTe ₂ O ₆ and PbVTeO ₅ F with Large Nonlinear-/Linear-Optical Responses due to Active Lone Pairs and Distorted Octahedra. Inorganic Chemistry, 2022, 61, 1538-1545.	1.9	10
6	Coordination units of Mn ²⁺ modulation toward tunable emission in zero-dimensional bromides for white light-emitting diodes. Journal of Materials Chemistry C, 2022, 10, 2095-2102.	2.7	35
7	<i>In situ</i> insertion of copper to form heteroanionic <i>D</i> _{3h} -symmetric [Cu ₃ Mo ₈ O ₃₂] ^{10â^²} for a templated Ag ₅₅ nanocluster. Nanoscale, 2022, 14, 4469-4473.	2.8	3
8	Engineering Steam Induced Surface Oxygen Vacancy onto Ni–Fe Bimetallic Nanocomposite for CO ₂ Electroreduction. Small, 2022, 18, e2108034.	5.2	20
9	Formamidinium Perovskitizers and Aromatic Spacers Synergistically Building Bilayer Dion–Jacobson Perovskite Photoelectric Bulk Crystals. ACS Applied Materials & Interfaces, 2022, 14, 11690-11698.	4.0	20
10	Organic–Inorganic High-Valence Sn ₁₈ -oxo Clusters: Direct Utilization of an Inorganic Sn(IV) Source to Improve the Nuclearity and Electrocatalytic CO ₂ Reduction Properties. Inorganic Chemistry, 2022, 61, 6037-6044.	1.9	6
11	Sequential enhancement of proton conductivity by aliovalent cadmium substitution and post-synthetic esterolysis in a carboxylate-functionalized indium framework with dimethylaminium templates. Inorganic Chemistry Frontiers, 2022, 9, 2997-3002.	3.0	4
12	Chemically anchoring molybdenum atoms onto micropore-rich VN nanosheet for boosted nitrogen electro-fixation via hydrogen bonds. Chemical Engineering Journal, 2022, 446, 136915.	6.6	4
13	Cdâ€Based Metal–Organic Framework for Selective Turnâ€On Fluorescent DMSO Residual Sensing. Chemistry - A European Journal, 2021, 27, 3753-3760.	1.7	12
14	Design and synthesis of PbBiVO5 electrode by polymorph engineering for rechargeable battery. Journal of Solid State Chemistry, 2021, 293, 121777.	1.4	1
15	Broadband white-light emission in a one-dimensional organic–inorganic hybrid cadmium chloride with face-sharing CdCl ₆ octahedral chains. Journal of Materials Chemistry C, 2021, 9, 88-94.	2.7	54
16	A <scp>Topâ€Down</scp> Approach towards Cu(I) Alkynyl Clusters with Unusual Geometry. Chinese Journal of Chemistry, 2021, 39, 937-941.	2.6	9
17	Blue luminescent N,S-doped carbon dots encapsulated in red emissive Eu-MOF to form dually emissive composite for reversible anti-counterfeit ink. Dalton Transactions, 2021, 50, 1690-1696.	1.6	19
18	Highly efficient self-trapped exciton emission in a one-dimensional face-shared hybrid lead bromide. Chemical Communications, 2021, 57, 2495-2498.	2.2	29

#	Article	IF	CITATIONS
19	Manipulation of Cl/Br transmutation in zero-dimensional Mn ²⁺ -based metal halides toward tunable photoluminescence and thermal quenching behaviors. Journal of Materials Chemistry C, 2021, 9, 2047-2053.	2.7	44
20	A lead-free layered Dion–Jacobson hybrid double perovskite constructed by an aromatic diammonium cation. Inorganic Chemistry Frontiers, 2021, 8, 3576-3580.	3.0	12
21	Turn-On Fluorescence Enantioselective Sensing of Hydroxyl Carboxylic Enantiomers by Metal–Organic Framework Nanosheets with a Homochiral Tetracarboxylate of Cyclohexane Diamide. ACS Applied Materials & Interfaces, 2021, 13, 20821-20829.	4.0	34
22	Engineering Oxygen Vacancies in Mesocrystalline CuO Nanosheets for Water Oxidation. ACS Applied Nano Materials, 2021, 4, 6135-6144.	2.4	22
23	Sr2Pb(BeB5O10)(BO3): An Excellent Ultraviolet Nonlinear-Optical Beryllium Borate by the Pb-Modified Construction of a Conjugated System and Lone-Pair Effect. Inorganic Chemistry, 2021, 60, 11214-11221.	1.9	10
24	Introducing High Density of Very Active Sites and Stepwise Postmodification for Tailoring the Porosity of Highly Demanding Cr ³⁺ -Based Metal–Organic Frameworks. Inorganic Chemistry, 2021, 60, 12109-12115.	1.9	3
25	<pre><scp>Fe₂Mn</scp>(<scp><i>μ</i>₃â€O</scp>)(<scp>COO</scp>)₆ Cluster Based Stable <scp>MOF</scp> for Oxidative Coupling of Amines via Heterometallic Synergy. Chinese Journal of Chemistry, 2021, 39, 2983-2989.</pre>	2.6	9
26	<i>In Situ</i> Aliovalent Nickle Substitution and Acidic Modification of Nanowalls Promoted Proton Conductivity in InOF with 1D Helical Channel. ACS Applied Materials & Interfaces, 2021, 13, 38289-38295.	4.0	9
27	Unraveling the Ultrafast Self-assembly and Photoluminescence in Zero-Dimensional Mn ²⁺ -Based Halides with Narrow-Band Green Emissions. ACS Applied Electronic Materials, 2021, 3, 4144-4150.	2.0	16
28	Insights into varying dimension structures for deep-UV optical crystals NaBa2Al(P2O7)2 and NaBaAl(PO4)2 constructed separately from unique [Al(P2O7)2] chains and [Al(PO4)2] layers. Journal of Solid State Chemistry, 2021, 301, 122333.	1.4	4
29	A Photochromic Zinc–Viologen Framework with a High-Contrast Nonlinear Optical Switchable Behavior. Crystal Growth and Design, 2021, 21, 5752-5759.	1.4	9
30	An uncoordinated tertiary nitrogen based tricarboxylate calcium network with Lewis acid–base dual catalytic sites for cyanosilylation of aldehydes. Dalton Transactions, 2021, 50, 1740-1745.	1.6	8
31	A One-Dimensional Broadband Emissive Hybrid Lead Iodide with Face-Sharing PbI ₆ Octahedral Chains. Inorganic Chemistry, 2021, 60, 15136-15140.	1.9	16
32	Two SbX5-based isostructural polar 1D hybrid antimony halides with tunable broadband emission, nonlinear optics, and semiconductor properties. Science China Chemistry, 2021, 64, 2111-2117.	4.2	10
33	Consolidation of 2D Frameworks Based on Corner-Shared Supertetrahedral T5 Clusters via M ₂ OS ₂ Units for Tunable Photoluminescent and Semiconductor Properties. Inorganic Chemistry, 2021, 60, 18307-18313.	1.9	2
34	Tandem Access to Acridones and their Fused Derivatives: [1+2+3] Annulation of Isocyanides with Unsaturated Carbonyls. Advanced Synthesis and Catalysis, 2020, 362, 2379-2384.	2.1	9
35	Optimized trimetallic benzotriazole-5-carboxylate MOFs with coordinately unsaturated active sites as an efficient electrocatalyst for the oxygen evolution reaction. Dalton Transactions, 2020, 49, 750-756.	1.6	25
36	Molecular‧ieving Membrane by Partitioning the Channels in Ultrafiltration Membrane by Inâ€Situ Polymerization. Angewandte Chemie - International Edition, 2020, 59, 4401-4405.	7.2	35

#	Article	IF	CITATIONS
37	A quasi-D3-symmetrical metal chalcogenide cluster constructed by the corner-sharing of two T3 supertetrahedra. Dalton Transactions, 2020, 49, 13958-13961.	1.6	5
38	Enhanced Proton Conductivity by Aliovalent Substitution of Cadmium for Indium in Dimethylaminium-Templated Metal Anilicates. ACS Applied Materials & Interfaces, 2020, 12, 41605-41612.	4.0	17
39	O-coordinated W-Mo dual-atom catalyst for pH-universal electrocatalytic hydrogen evolution. Science Advances, 2020, 6, eaba6586.	4.7	263
40	Tri(pyridinyl)pyridine Viologen-Based Kagome Dual Coordination Polymer with Selective Chromic Response to Soft X-ray and Volatile Organic Amines. Inorganic Chemistry, 2020, 59, 9047-9054.	1.9	40
41	M ₄ LiBe ₄ P ₇ O ₂₄ and M ₄ Li(Li ₃ P)P ₇ O ₂₄ (M = Cs, Rb): deep-ultraviolet nonlinear-optical phosphates with a tetrahedra-substituted paracelsian-like framework. Chemical Communications. 2020. 56. 8639-8642.	2.2	7
42	BaLiTe ₂ O ₅ X (X = Cl, Br): mixed alkali/alkaline-earth metal tellurite halides with [Te ₂ O ₅] _{â^ž} chains. Dalton Transactions, 2020, 49, 4914-4919.	1.6	7
43	Covalently Connected Nb ₄ N _{5–<i>x</i>} O _{<i>x</i>} –MoS ₂ Heterocatalysts with Desired Electron Density to Boost Hydrogen Evolution. ACS Nano, 2020, 14, 4925-4937.	7.3	50
44	Front Cover Picture: Tandem Access to Acridones and their Fused Derivatives: [1+2+3] Annulation of Isocyanides with Unsaturated Carbonyls (Adv. Synth. Catal. 12/2020). Advanced Synthesis and Catalysis, 2020, 362, 2287-2287.	2.1	0
45	A triflate and alkynyl protected Ag43 nanocluster with a passivated surface. RSC Advances, 2020, 10, 19397-19400.	1.7	2
46	High Coordinate Metal lodate Chlorides with Diverse Structural Motifs and Tunable Birefringence. Crystal Growth and Design, 2020, 20, 5473-5483.	1.4	8
47	Modulator-Induced Zr-MOFs Diversification and Investigation of Their Properties in Gas Sorption and Fe3+ Ion Sensing. Inorganic Chemistry, 2020, 59, 2961-2968.	1.9	22
48	Observation of Nonâ€FCC Copper in Alkynylâ€Protected Cu ₅₃ Nanoclusters. Angewandte Chemie, 2020, 132, 6569-6574.	1.6	6
49	Tetrahedral μ ₄ -chloride and <i>in situ</i> generated octahedral μ ₆ -sulfide templating Co ₈ complexes with different distortions of the cube. Chemical Communications, 2020, 56, 4236-4239.	2.2	5
50	The construction of helicate metal–organic nanotubes and enantioselective recognition. Journal of Materials Chemistry C, 2020, 8, 4453-4460.	2.7	12
51	A rational design of efficient trifunctional electrocatalysts derived from tailored Co ²⁺ -functionalized anionic metal–organic frameworks. Dalton Transactions, 2020, 49, 2280-2289.	1.6	14
52	Observation of Nonâ€FCC Copper in Alkynylâ€Protected Cu ₅₃ Nanoclusters. Angewandte Chemie - International Edition, 2020, 59, 6507-6512.	7.2	56
53	A pre-synthetic strategy to construct single ion conductive covalent organic frameworks. Chemical Communications, 2020, 56, 2747-2750.	2.2	29
54	A two-dimensional bilayered Dion–Jacobson-type perovskite hybrid with a narrow bandgap for broadband photodetection. Inorganic Chemistry Frontiers, 2020, 7, 1394-1399.	3.0	25

#	Article	IF	CITATIONS
55	A series of silver doped butterfly-like Ti ₈ Ag ₂ clusters with two Ag ions panelled on a Ti ₈ surface. Dalton Transactions, 2019, 48, 13423-13429.	1.6	26
56	X-ray and UV Dual Photochromism, Thermochromism, Electrochromism, and Amine-Selective Chemochromism in an Anderson-like Zn ₇ Cluster-Based 7-Fold Interpenetrated Framework. Journal of the American Chemical Society, 2019, 141, 12663-12672.	6.6	248
57	LiM ^{II} (IO ₃) ₃ (M ^{II} =Zn and Cd): Two Promising Nonlinear Optical Crystals Derived from a Tunable Structure Model of αâ€LiIO ₃ . Angewandte Chemie, 2019, 131, 17354-17358.	1.6	49
58	LiM ^{II} (IO ₃) ₃ (M ^{II} =Zn and Cd): Two Promising Nonlinear Optical Crystals Derived from a Tunable Structure Model of αâ€LiIO ₃ . Angewandte Chemie - International Edition, 2019, 58, 17194-17198.	7.2	69
59	BeO ₆ Trigonal Prism with Ultralong Be–O Bonds Observed in a Deep Ultraviolet Optical Crystal Li ₁₃ BeBe ₆ B ₉ O ₂₇ . Inorganic Chemistry, 2019, 58, 2201-2207.	1.9	9
60	KBi(IO ₃) ₃ (OH) and NaBi(IO ₃) ₄ : from the centrosymmetric chain to a noncentrosymmetric double layer. Dalton Transactions, 2019, 48, 10320-10326.	1.6	15
61	A superstable 3p-block metal–organic framework platform towards prominent CO ₂ and C1/C2-hydrocarbon uptake and separation performance and strong Lewis acid catalysis for CO ₂ fixation. Inorganic Chemistry Frontiers, 2019, 6, 813-819.	3.0	45
62	Highly Selective Radioactive ¹³⁷ Cs ⁺ Capture in an Open-Framework Oxysulfide Based on Supertetrahedral Cluster. Chemistry of Materials, 2019, 31, 1628-1634.	3.2	30
63	Single-Component Color-Tunable Gd(pic) ₃ : Eu ³⁺ Phosphor Based on a Metal–Organic Framework for Near-UV White-Light-Emitting Diodes. ACS Omega, 2019, 4, 3593-3600.	1.6	15
64	Coexistence of Cu(<scp>ii</scp>) and Cu(<scp>i</scp>) in Cu ion-doped zeolitic imidazolate frameworks (ZIF-8) for the dehydrogenative coupling of silanes with alcohols. Dalton Transactions, 2019, 48, 16562-16568.	1.6	37
65	Precise and Wide-Ranged Band-Gap Tuning of Ti ₆ -Core-Based Titanium Oxo Clusters by the Type and Number of Chromophore Ligands. Inorganic Chemistry, 2019, 58, 16785-16791.	1.9	39
66	The photochromic behaviour of two viologen salts modulated by the distances between the halide anions and the cationic N atoms of viologen. Acta Crystallographica Section C, Structural Chemistry, 2019, 75, 1628-1634.	0.2	6
67	(003)-Facet-exposed Ni3S2 nanoporous thin films on nickel foil for efficient water splitting. Applied Catalysis B: Environmental, 2019, 243, 693-702.	10.8	129
68	Synergetic Influence of Alkali-Metal and Lone-Pair Cations on Frameworks of Tellurites. Inorganic Chemistry, 2018, 57, 5406-5412.	1.9	13
69	Chiral metal–organic frameworks constructed from four-fold helical chain SBUs for enantioselective recognition of α-hydroxy/amino acids. Inorganic Chemistry Frontiers, 2018, 5, 153-159.	3.0	26
70	Defect-enriched iron fluoride-oxide nanoporous thin films bifunctional catalyst for water splitting. Nature Communications, 2018, 9, 1809.	5.8	188
71	Silverâ€Catalyzed Isocyanide Insertion into Nâ^'H Bond of Ammonia: [5+1] Annulation to Quinazoline Derivatives. Advanced Synthesis and Catalysis, 2018, 360, 1938-1942.	2.1	27
72	Li6Na3Sr14Al11P22O90: an oxo-centered Al3cluster based phosphate constructed from two types of (3,6)-connected kgd layers. Dalton Transactions, 2018, 47, 298-301.	1.6	7

#	Article	IF	CITATIONS
73	Breathing Europium–Terbium Co-doped Luminescent MOF as a Broad-Range Ratiometric Thermometer with a Contrasting Temperature–Intensity Relationship. ACS Omega, 2018, 3, 5754-5760.	1.6	28
74	Photochromic Porous and Nonporous Viologen-Based Metal–Organic Frameworks for Visually Detecting Oxygen. Crystal Growth and Design, 2018, 18, 3883-3889.	1.4	65
75	Cobalt nanocrystals embedded into N-doped carbon as highly active bifunctional electrocatalysts from pyrolysis of triazolebenzoate complex. Electrochimica Acta, 2018, 284, 733-741.	2.6	13
76	Novel Covalent Triazine Framework for High-Performance CO ₂ Capture and Alkyne Carboxylation Reaction. ACS Applied Materials & Interfaces, 2018, 10, 27972-27978.	4.0	78
77	Reversible Double Nucleophilic Substitution Reaction inside Single-Crystal MOF Tuned Remarkable Magnetic Behavior. Inorganic Chemistry, 2018, 57, 6787-6790.	1.9	12
78	Light and Heat Dually Responsive Luminescence in Organic Templated CdSO ₄ -type Halogeno(cyano)cuprates with Disorder of Halogenide/Cyanide. Crystal Growth and Design, 2017, 17, 746-752.	1.4	20
79	A Fluorescent Anionic MOF with Zn ₄ (trz) ₂ Chain for Highly Selective Visual Sensing of Contaminants: Cr(III) Ion and TNP. Inorganic Chemistry, 2017, 56, 2690-2696.	1.9	129
80	Solventâ€Assisted Metal Metathesis: A Highly Efficient and Versatile Route towards Synthetically Demanding Chromium Metal–Organic Frameworks. Angewandte Chemie, 2017, 129, 6578-6582.	1.6	4
81	Innentitelbild: Solventâ€Assisted Metal Metathesis: A Highly Efficient and Versatile Route towards Synthetically Demanding Chromium Metal–Organic Frameworks (Angew. Chem. 23/2017). Angewandte Chemie, 2017, 129, 6444-6444.	1.6	0
82	One-step ethanolysis of lignin into small-molecular aromatic hydrocarbons over nano-SiC catalyst. Bioresource Technology, 2017, 226, 145-149.	4.8	22
83	Tunability in Metal Coordination Sphere, Ligand Coordination Mode, Network Topology, and Magnetism via Stepwise Dehydration Induced Single-Crystal to Single-Crystal Transformation. Crystal Growth and Design, 2017, 17, 3724-3730.	1.4	12
84	Heptazine-Based Porous Framework Supported Palladium Nanoparticles for Green Suzuki–Miyaura Reaction. Industrial & Engineering Chemistry Research, 2017, 56, 4275-4280.	1.8	33
85	Solventâ€Assisted Metal Metathesis: A Highly Efficient and Versatile Route towards Synthetically Demanding Chromium Metal–Organic Frameworks. Angewandte Chemie - International Edition, 2017, 56, 6478-6482.	7.2	80
86	Two Phosphates: Noncentrosymmetric Cs ₆ Mg ₆ (PO ₃) ₁₈ and Centrosymmetric Cs ₂ MgZn ₂ (P ₂ O ₇) ₂ . Inorganic Chemistry, 2017, 56, 845-851.	1.9	48
87	Alkali earth MO _x (<i>x</i> = 6, 7, 9, 12) polyhedra tuned cadmium selenites with different dimensions and diverse SeO ₃ ^{2â~} coordinations. CrystEngComm, 2017, 19, 6644-6650.	1.3	1
88	Observation of Contrary Thermo-responsive Trend for Single Crystal and Powder Samples in Mechano-, Thermo- and Solvato-responsive Luminescent Cubane [Ag4I4L4] Cluster. Scientific Reports, 2017, 7, 13058.	1.6	12
89	Bidentate Phosphine-Assisted Synthesis of an All-Alkynyl-Protected Ag ₇₄ Nanocluster. Journal of the American Chemical Society, 2017, 139, 12346-12349.	6.6	148
90	Fourfold-Interpenetrated MOF [Ni(pybz) ₂] as Coating Material in Gas Chromatographic Capillary Column for Separation. Inorganic Chemistry, 2017, 56, 8912-8919.	1.9	16

#	Article	IF	CITATIONS
91	Heterogeneous hybrid of propyl amino functionalized MCM-41 and 1 <i>H</i> -1,2,4-triazole for high efficient intermediate temperature proton conductor. RSC Advances, 2017, 7, 52321-52326.	1.7	4
92	Unveiling the relative stability and proton binding of non-classical Wells–Dawson isomers of [(NaF6)W18O54(OH)2]7â~' and [(SbO6)W18O54(OH)2]9â~': a DFT study. Dalton Transactions, 2017, 46, 16145-16158.	1.6	3
93	Pb@Pb ₈ Basket-like-Cluster-Based Lead Tellurate–Nitrate Kleinman-Forbidden Nonlinear-Optical Crystal: Pb ₉ Te ₂ O ₁₃ (OH)(NO ₃) ₃ . Inorganic Chemistry. 2017. 56. 7900-7906.	1.9	26
94	Homochiral MOF as Circular Dichroism Sensor for Enantioselective Recognition on Nature and Chirality of Unmodified Amino Acids. ACS Applied Materials & Interfaces, 2017, 9, 20991-20999.	4.0	91
95	Carbazolic Porous Framework with Tetrahedral Core for Gas Uptake and Tandem Detection of Iodide and Mercury. ACS Applied Materials & amp; Interfaces, 2017, 9, 21438-21446.	4.0	41
96	Phase Transfer of Nanoparticles Using an Amphiphilic Ionic Liquid. Langmuir, 2016, 32, 13746-13751.	1.6	11
97	Open-Framework Oxysulfide Based on the Supertetrahedral [In ₄ Sn ₁₆ O ₁₀ S ₃₄] ^{12–} Cluster and Efficient Sequestration of Heavy Metals. Journal of the American Chemical Society, 2016, 138, 5543-5546.	6.6	99
98	Photochromic and Nonphotochromic Luminescent Supramolecular Isomers Based on Carboxylate-Functionalized Bipyridinium Ligand: (4,4)-Net versus Interpenetrated (6,3)-Net. ACS Applied Materials & Interfaces, 2016, 8, 24862-24869.	4.0	79
99	Flexible solid-state supercapacitor of metal-organic framework coated on carbon nanotube film interconnected by electrochemically -codeposited PEDOT-GO. ChemistrySelect, 2016, 1, 285-289.	0.7	60
100	Single Component Lanthanide Hybrids Based on Metal–Organic Framework for Near-Ultraviolet White Light LED. ACS Applied Materials & Interfaces, 2016, 8, 24123-24130.	4.0	99
101	A Luminescent Zinc(II) Metal–Organic Framework (MOF) with Conjugated ï€-Electron Ligand for High Iodine Capture and Nitro-Explosive Detection. Inorganic Chemistry, 2016, 55, 9270-9275.	1.9	176
102	Tandem cycloaddition–decarboxylation of α-keto acid and isocyanide under oxidant-free conditions towards monosubstituted oxazoles. RSC Advances, 2016, 6, 73450-73453.	1.7	13
103	Simultaneous Luminescent Thermochromism, Vapochromism, Solvatochromism, and Mechanochromism in a <i>C</i> ₃ -Symmetric Cubane [Cu ₄ I ₄ P ₄] Cluster without Cu–Cu Interaction. Inorganic Chemistry, 2016, 55, 7323-7325.	1.9	79
104	In Situ Surface Engineering of Mesoporous Silica Generates Interfacial Activity and Catalytic Acceleration Effect. ACS Omega, 2016, 1, 930-938.	1.6	10
105	KSbI 6 O 18 : An antimony iodate semiconductor material with cyclic chiral S 6 -symmetric hexaiodate. Inorganic Chemistry Communication, 2016, 65, 13-15.	1.8	5
106	Cyanide-bridged mixed-valence copper(II/I) coordination polymers: Unique 7-connected sev-type 3D network versus anionic 2D host network encapsulated with cationic complex. Inorganic Chemistry Communication, 2016, 63, 101-106.	1.8	8
107	Hexagonal Co ₆ and zigzag Co ₄ cluster based magnetic MOFs with a pcu net for selective catalysis. Inorganic Chemistry Frontiers, 2016, 3, 78-85.	3.0	8
108	Genuine supramolecular isomers based on Y-shaped pyridinedicarboxylate ligands with distinct topology: 2D 6 ³ layer, kgd layer to 3D rtl net. CrystEngComm, 2016, 18, 2065-2071.	1.3	13

#	Article	IF	CITATIONS
109	Enhanced Selective CO2 Capture upon Incorporation of Dimethylformamide in the Cobalt Metal–Organic Framework [Co3(OH)2(btca)2]. Energy & Fuels, 2016, 30, 526-530.	2.5	11
110	Efficient and environmentally friendly Glaser coupling of terminal alkynes catalyzed by multinuclear copper complexes under base-free conditions. RSC Advances, 2016, 6, 28653-28657.	1.7	22
111	An azo-linked porous triptycene network as an absorbent for CO ₂ and iodine uptake. Polymer Chemistry, 2016, 7, 643-647.	1.9	123
112	Solvent-free heterogeneous catalysis for cyanosilylation in a modified sodalite-type Cu(<scp>ii</scp>)-MOF. RSC Advances, 2015, 5, 24293-24298.	1.7	29
113	A homochiral magnet based on D ₃ symmetric [(NaO ₃)Co ₃] clusters: from spontaneous resolution to absolute chiral induction. Chemical Communications, 2015, 51, 5108-5111.	2.2	31
114	Enhanced Catalysis Activity in a Coordinatively Unsaturated Cobalt-MOF Generated via Single-Crystal-to-Single-Crystal Dehydration. Inorganic Chemistry, 2015, 54, 6312-6318.	1.9	45
115	An non-centrosymmetric mononuclear Zr complex exhibiting UV second-harmonic-generation. Functional Materials Letters, 2015, 08, 1550029.	0.7	0
116	Heptazine-Based Porous Framework for Selective CO ₂ Sorption and Organocatalytic Performances. ACS Applied Materials & Interfaces, 2015, 7, 28452-28458.	4.0	51
117	A New Class of Cuprous Bromide Cluster-Based Hybrid Materials: Direct Observation of the Stepwise Replacement of Hydrogen Bonds by Coordination Bonds. Inorganic Chemistry, 2015, 54, 554-559.	1.9	19
118	An interpenetrated bioactive nonlinear optical MOF containing a coordinated quinolone-like drug and Zn(<scp>ii</scp>) for pH-responsive release. Dalton Transactions, 2015, 44, 1800-1804.	1.6	47
119	A perfectly aligned 6 ₃ helical tubular cuprous bromide single crystal for selective photo-catalysis, luminescence and sensing of nitro-explosives. Dalton Transactions, 2015, 44, 3410-3416.	1.6	12
120	Solvent-free heterogeneous catalysis for cyanosilylation in a dynamic cobalt-MOF. Dalton Transactions, 2015, 44, 12711-12716.	1.6	54
121	Pb ₇ O(OH) ₃ (CO ₃) ₃ (BO ₃): First Mixed Borate and Carbonate Nonlinear Optical Material Exhibiting Large Second-Harmonic Generation Response. Inorganic Chemistry, 2015, 54, 4138-4142.	1.9	69
122	Planar Mn ₄ O Cluster Homochiral Metal–Organic Framework for HPLC Separation of Pharmaceutically Important (±)-Ibuprofen Racemate. Inorganic Chemistry, 2015, 54, 3713-3715.	1.9	66
123	An organic-ligand-free thermochromic luminescent cuprous iodide trinuclear cluster: evidence for cluster centered emission and configuration distortion with temperature. Chemical Communications, 2015, 51, 8062-8065.	2.2	80
124	A pyridyl-decorated MOF-505 analogue exhibiting hierarchical porosity, selective CO2 capture and catalytic capacity. Dalton Transactions, 2015, 44, 20027-20031.	1.6	14
125	Reversible single-crystal-to-single-crystal transformation from a mononuclear complex to a fourfold interpenetrated MOF with selective adsorption of CO ₂ . Dalton Transactions, 2015, 44, 19796-19799.	1.6	19
126	Three-coordinate copper(I) 2-hydroxy-1,10-phenanthroline dinuclear complex catalyzed homocoupling of arylboronic acids towards biphenyls under air condition. Tetrahedron, 2015, 71, 9598-9601.	1.0	14

#	Article	IF	CITATIONS
127	Selective adsorption in two porous triazolate–oxalate-bridged antiferromagnetic metal-azolate frameworks obtained via in situ decarboxylation of 3-amino-1,2,4-triazole-5-carboxylic acid. Journal of Solid State Chemistry, 2015, 223, 73-78.	1.4	9
128	Ferromagnetically coupled chiral dysprosium hydroxysulfate and centrosymmetric dysprosium hydroxysulfate-oxalate: Dy ₄ (OH) ₄ cubane based high-connected networks via in situ conversion of organosulfur to sulfate. RSC Advances, 2014, 4, 53954-53959.	1.7	13
129	Tunable Nonlinear Optical Property and Photocatalytic Activity on Luminescent Chiral Lanthanide Chains. Chinese Journal of Chemistry, 2014, 32, 1259-1266.	2.6	3
130	Planar Cu2(ppz)2 Dimers as SBUs for Diverse Polyoxometalate-Based Metal Organic Frameworks. Crystal Growth and Design, 2014, 14, 5773-5783.	1.4	6
131	Luminescent group 12 metal tetracarboxylate networks as probe for metal ions. RSC Advances, 2014, 4, 49090-49097.	1.7	20
132	Tuning of Valence States, Bonding Types, Hierarchical Structures, and Physical Properties in Copper/Halide/Isonicotinate System. Inorganic Chemistry, 2014, 53, 4130-4143.	1.9	39
133	A Single-Chain Magnet Based on {Co ^{II} ₄ } Complexes and Azido/Picolinate Ligands. Inorganic Chemistry, 2014, 53, 7870-7875.	1.9	23
134	Cu ₃ I ₇ Trimer and Cu ₄ I ₈ Tetramer Based Cuprous Iodide Polymorphs for Efficient Photocatalysis and Luminescent Sensing: Unveiling Possible Hierarchical Assembly Mechanism. Inorganic Chemistry, 2014, 53, 8376-8383.	1.9	90
135	Mixed CoN4Cl2 and CoCl4 units versus two CoN2Cl3 units in [Co2(Htbi)2Cl4] isomers. Inorganic Chemistry Communication, 2014, 39, 21-25.	1.8	6
136	From (3,6)-Connected kgd, chiral anh to (3,8)-connected tfz-d Nets in Low Nuclear Metal Cluster-Based Networks with Triangular Pyridinedicarboxylate Ligand. Crystal Growth and Design, 2013, 13, 1618-1625.	1.4	34
137	(H2en)0.5[BiO(OH)2(H2O)]: The first organic templated layered bismuthate. Inorganic Chemistry Communication, 2013, 30, 133-135.	1.8	5
138	Cuprous Halide Coordination Polymers Based on Cationic [Cu4X2] and [Cu3X] Clusters and [Cu2Br]nLayers with Tetrazolates as Assembling Ligands: Highly Connected Networks and Halide-Dependent Luminescence. European Journal of Inorganic Chemistry, 2013, 2013, 556-562.	1.0	23
139	Triangle, square and delta-chain based cobalt tetrazolate magnets. Dalton Transactions, 2013, 42, 6611.	1.6	56
140	Mn8@Na8 Cube-in-Cube SBBs-Based Heterometallic Coordination Network with Unprecedented (39.46)8 Topological Mn8(μ4-OMe)6 Cubes. Crystal Growth and Design, 2013, 13, 1386-1389.	1.4	3
141	Photoluminescent cuprous iodide polymorphs generated via in situ organic reactions. Inorganic Chemistry Communication, 2013, 32, 12-17.	1.8	15
142	Heterometallic Mixedâ€Valence Copper(I,II) Cyanides that were Tuned by Using the Chelate Effect: Discovery of Famous Cairo Pentagonal Tiling and Unprecedented (3,4)â€Connected {8 ³ } ₂ {8 ⁶ } Topological 3D Net. Chemistry - an Asian Journal, 2013, 8, 1587-1595.	1.7	13
143	Rung-defected ladder of azido-bridged Cu(ii) chains linked by [Cu(picolinate)2] units. Dalton Transactions, 2013, 42, 11571.	1.6	16
144	Reconstruction of a (6,3) Brick Wall Sheet Giving an Unprecedented Shubnikov-type (5,34) Sheet in Luminescent Cuprous Cyanide Supramolecular Isomers of Pseudo-polyrotaxane. Crystal Growth and Design, 2012, 12, 6068-6073.	1.4	27

#	Article	IF	CITATIONS
145	A Unique Solventâ€Induced Structural Transformation of Two Acentric [Zn ₂ (H ₂ O)(Hdtim) ₂] Isomers. Chinese Journal of Chemistry, 2012, 30, 2232-2236.	2.6	4
146	Three novel Bi(<scp>iii</scp>) complexes with in situ generated anilate ligands: unusual oxidation of cyclohexanedione to dihydroxy benzoquinone. Dalton Transactions, 2012, 41, 1562-1567.	1.6	16
147	Magnetic Modulation and Cation-Exchange in a Series of Isostructural (4,8)-Connected Metal–Organic Frameworks with Butterfly-like [M ₄ (OH) ₂ (RCO ₂) ₈] Building Units. Chemistry of Materials. 2012. 24. 303-310.	3.2	62
148	Organic Templated Cuprous Cyanide Open Frameworks Based on Cu2(CN)6Dimer with Strong and Long-Lived Luminescence. Crystal Growth and Design, 2011, 11, 3101-3108.	1.4	29
149	A Perfectly Square-Planar Tetracoordinated Oxygen in a Tetracopper Cluster-Based Coordination Polymer. Journal of the American Chemical Society, 2011, 133, 4788-4790.	6.6	65
150	Solvent induced molecular magnetic changes observed in single-crystal-to-single-crystal transformation. Dalton Transactions, 2011, 40, 2092.	1.6	47
151	Spin Canting and Metamagnetism in the First Hybrid Cobalt–Hypoxanthine Open Framework with <i>umr</i> Topology. Chemistry - A European Journal, 2011, 17, 5588-5594.	1.7	41
152	Spin canting in a novel (3,4)-connected mixed-valence cobalt coordination polymer based on oxalates and [Co(Hbiim)3] (H2biim=2,2′-biimidazole) building blocks. Inorganic Chemistry Communication, 2010, 13, 1100-1102.	1.8	10
153	In situ alkylation of N-heterocycles in organic templated cuprous halides. Dalton Transactions, 2010, 39, 2701.	1.6	49
154	A DFT Study on the Mechanism of the Coupling Reaction between Chloromethyloxirane and Carbon Dioxide Catalyzed by Re(CO) ₅ Br. Organometallics, 2010, 29, 2069-2079.	1.1	30
155	Red phosphorescent cuprous halide/pseudohalide coordination polymers with pyrimidine-2-thionates as Co-ligands. CrystEngComm, 2010, 12, 1103-1109.	1.3	21
156	Structure and Stability of Endohedral X@C60F, X@C60F2 (X = N, H), and (H@C60)2. Journal of Physical Chemistry C, 2010, 114, 7558-7562.	1.5	2
157	P6Mo18O73 heteropolyanion and its four-copper complex: theoretical and experimental investigation. Dalton Transactions, 2010, 39, 8256.	1.6	22
158	Enantiomers of conformation-flexible cyclopentane-1,2,3,4-tetracarboxylate in metal–organic frameworks. CrystEngComm, 2010, 12, 4416.	1.3	10
159	A hybrid cobalt hydroxyacetate magnet: ionothermal synthesis, 3-D Co–O–Co connectivity and spin glass behavior. Dalton Transactions, 2010, 39, 1179-1181.	1.6	6
160	Luminescent boracite-like metal–organic frameworks constructed by Cu-centered CuCu4 tetrahedra and CuCu3 triangles with an acentric cubic superlarge cell. CrystEngComm, 2010, 12, 55-58.	1.3	15
161	Theoretical study on the mechanism of nickel(0)-mediated coupling between carbon dioxide and epoxyethane. Computational and Theoretical Chemistry, 2009, 916, 125-134.	1.5	26
162	A luminescent [Ag3S3]n-tube based metal–organic framework. Inorganic Chemistry Communication, 2009, 12, 375-377.	1.8	16

#	Article	IF	CITATIONS
163	Spin Frustration and Long-Range Ordering in an AlB2-like Metal-Organic Framework with Unprecedented N,N,N-Tris-tetrazol-5-yl-amine Ligand. Inorganic Chemistry, 2009, 48, 4536-4541.	1.9	49
164	<i>D</i> ₃ -Symmetric Supramolecular Cation {(Me ₂ NH ₂) ₆ (SO ₄)} ⁴⁺ As a New Template for 3D Homochiral (10,3)-a Metal Oxalates. Crystal Growth and Design, 2009, 9, 1702-1707.	1.4	43
165	Hybrid Cobalt Hydroxyoxalate Material Containing 3D Coâ^'Oâ^'Co Connectivity and Showing Ferrimagnetic Ordering. Inorganic Chemistry, 2008, 47, 7462-7464.	1.9	21
166	Cu6S4 Cluster Based Twelve-Connected Face-Centered Cubic and Cu19I4S12 Cluster Based Fourteen-Connected Body-Centered Cubic Topological Coordination Polymers. Inorganic Chemistry, 2008, 47, 8197-8203.	1.9	51
167	Two Cuprous Cyanide Polymorphs: Diamond Net versus 3,4-Connected Net. Inorganic Chemistry, 2008, 47, 2255-2257.	1.9	30
168	Phosphorescent Acentric Cuprous Halide Coordination Polymers for Nolinear Optical Materials. Crystal Growth and Design, 2008, 8, 2359-2363.	1.4	14
169	Tube and Cage C ₆₀ H ₆₀ : A Comparison with C ₆₀ F ₆₀ . Organic Letters, 2008, 10, 2573-2576.	2.4	12
170	Fused Five-Membered Rings Determine the Stability of C ₆₀ F ₆₀ . Journal of the American Chemical Society, 2008, 130, 3985-3988.	6.6	39
171	Unusual Slow Magnetic Relaxation in Helical Co3(OH)2 Ferrimagnetic Chain Based Cobalt Hydroxysulfates. Chemistry of Materials, 2008, 20, 2298-2305.	3.2	33
172	Temperature Tuned Synthesis of Zinc <i>N</i> , <i>N</i> -bis-(1(2)H-tetrazol-5-yl)-amine Complexes: From Zn ₃ O Cluster-Based 3-Connected 6 ³ - <i>hcb</i> and (3,6)-Connected (4 ³) ₂ (4 ⁶)- <i>kgd</i> Layers to Zn ₅ (OH) ₄ Chain-Based 3D Open Framework. Crystal Growth and Design, 2008, 8, 3077-3083.	1.4	54
173	Structural and Electronic Properties of Hetero-Transition-Metal Keggin Anions:Â A DFT Study of αJβ-[XW12O40]n-(X = CrVI, VV, TiIV, FeIII, CoIII, NiIII, CoII, and ZnII) Relative Stability. Journal of Physical Chemistry A, 2007, 111, 159-166.	1.1	24
174	Inversed Stability Order in Keggin Polyoxothiometalate Isomers: A DFT Study of 12-Electron Reduced α, β, γ, Ĩ´, and Îμ [(MoO4)Mo12O12S12(OH)12]2-Anions. Journal of Physical Chemistry A, 2007, 111, 1683-1687.	1.1	10
175	Ligand Concentration Controlled Supramolecular Isomerism in Two CuSCN Based Coordination Polymers with in Situ Synthesized 4,4â€~-Dipyridylsulfide as a Co-Ligand. Crystal Growth and Design, 2007, 7, 64-68.	1.4	90
176	Unprecedented (3,9)-Connected (42.6)3(46.621.89) Net Constructed by Trinuclear Mixed-Valence Cobalt Clusters. Crystal Growth and Design, 2007, 7, 980-983.	1.4	130
177	Dehydration-Induced Conversion from a Single-Chain Magnet into a Metamagnet in a Homometallic Nanoporous Metal–Organic Framework. Angewandte Chemie - International Edition, 2007, 46, 3456-3459.	7.2	231
178	Blue-green photoluminescent 5- and 10-connected metal 5-(4′-carboxy-phenyl)tetrazolate coordination polymers. Inorganic Chemistry Communication, 2007, 10, 1194-1197.	1.8	58
179	Double salts of copper(I) chloride incorporated hydroxylpyrimidine and tetrazole ligands. Inorganica Chimica Acta, 2007, 360, 14-20.	1.2	23
180	Two Mixed-Valence Vanadium(III,IV) Phosphonoacetates with 16-Ring Channels: H2(DABCO)[VIVO(H2O)VIII(OH)(O3PCH2CO2)2]·2.5H2O and H2(PIP)[VIVO(H2O)VIII(OH)(O3PCH2CO2)2]·2.5H2O. Inorganic Chemistry, 2006, 45, 8120-8125.	1.9	32

#	Article	IF	CITATIONS
181	Diversity of Coordination Architecture of Metal 4,5-Dicarboxyimidazole. Inorganic Chemistry, 2006, 45, 4801-4810.	1.9	234
182	Structures and Magnetic Properties of a Series of Metal Phosphonoacetates Synthesized from in Situ Hydrolysis of Triethyl Phosphonoacetate. Crystal Growth and Design, 2006, 6, 1445-1452.	1.4	31
183	A NaCl-like Metalâ^'Organic Framework Constructed by Unprecedented Tetrahedral Cd4O6 and Cd5O6 Units. Crystal Growth and Design, 2006, 6, 2637-2639.	1.4	42
184	One-dimensional cobalt and zinc complexes involving in situ reaction of ethylenediamine and acetonitrile to form imidazoline ligand. Inorganic Chemistry Communication, 2006, 9, 57-59.	1.8	12
185	Syntheses and structures of two copper–molybdate complexes: The 3-D [Cu(4,4′-bpy)(MoO4)] and 1-D [Cu2(HDABCO)2(H2Mo8O27)]·4H2O. Inorganica Chimica Acta, 2006, 359, 2023-2028.	1.2	11
186	In situ alkylation of 4,4′-bipyridine in hydrothermal synthesis of one-dimensional copper(I) bromide compounds. Inorganica Chimica Acta, 2006, 359, 3991-3995.	1.2	36
187	Syntheses and structures of metal tetrazole coordination polymers. Dalton Transactions, 2006, , 3170.	1.6	140
188	Syntheses, structures and properties of three metal pyridinecarboxylates. Inorganica Chimica Acta, 2005, 358, 1865-1872.	1.2	14
189	Insight into the structure and intrinsic stability of the Keggin and Wells-Dawson neutral cages. Computational and Theoretical Chemistry, 2005, 755, 119-126.	1.5	9
190	Hydro(solvo)thermal in situ ligand syntheses. Coordination Chemistry Reviews, 2005, 249, 1201-1219.	9.5	539
191	Di-μ-chloro-bis[bis(ethane-1,2-diamine-lº2N,N′)manganese(II)] dichloride. Acta Crystallographica Section E: Structure Reports Online, 2005, 61, m973-m974.	0.2	1
192	Langbeinite-type (NH4)2Mn2(SO4)3. Acta Crystallographica Section E: Structure Reports Online, 2005, 61, i82-i83.	0.2	0
193	μ-4,4′-Bipyridine-κ2N:N′-bis[triaqua(pyridine-2,4-dicarboxylato-κ2N,O)cobalt(II)] dihydrate. Acta Crystallographica Section E: Structure Reports Online, 2005, 61, m1332-m1333.	0.2	0
194	Hexakis(1-oxido-1H-benzotriazol-3-ium-κO)iron(III) tris(perchlorate) acetonitrile disolvate. Acta Crystallographica Section E: Structure Reports Online, 2005, 61, m1799-m1800.	0.2	6
195	Bis(hexane-1,6-diaminium) di-μ5-hydrogenphosphato-penta-μ2-oxo-pentakis[dioxomolybdenum(VI)] dihydrate. Acta Crystallographica Section E: Structure Reports Online, 2005, 61, m1933-m1934.	0.2	1
196	New double-layered open metal–organic frameworks with nanosized channels encapsulated removable 2,5-bis(4-pyridyl)-1,3,4-thiadiazole molecules. CrystEngComm, 2005, 7, 96-101.	1.3	22
197	Cuprophilicity-Induced Cocrystallization of [Cu2(4,4â€ [~] -bpy)(CN)2]nSheets and [Cu(SCN)]nChains into a 3-D Pseudopolyrotaxane. Inorganic Chemistry, 2005, 44, 7301-7303.	1.9	45
198	Extended Water Tapes of Cyclic Hexamers Encapsulated in the Channels of a Metal Phosphonocarboxylate Network. Crystal Growth and Design, 2005, 5, 1335-1337.	1.4	69

#	Article	IF	CITATIONS
199	Hydrothermal Syntheses and Structures of Two Mixed-Valence Copper(I,II) 2-Pyrazinecarboxylate Coordination Polymers. Inorganic Chemistry, 2005, 44, 3955-3959.	1.9	78
200	A Twelve-Connected Cu6S4Cluster-Based Coordination Polymer. Journal of the American Chemical Society, 2005, 127, 7670-7671.	6.6	246
201	trans-Diaquabis(1H-imidazole-4,5-dicarboxylato-κ2N3,O4)cadmium(II). Acta Crystallographica Section E: Structure Reports Online, 2004, 60, m12-m13.	0.2	4
202	catena-Poly[bis[(2,2′-bipyridine-κ2N,N′)manganese(II)]-di-μ-4-hydroxyisophthalato]. Acta Crystallographica Section E: Structure Reports Online, 2004, 60, m50-m52.	0.2	2
203	Tetraaquabis(4-pyridylthioacetato)nickel(II). Acta Crystallographica Section E: Structure Reports Online, 2004, 60, m135-m136.	0.2	3
204	Bis(3,5-dimethylpiperazinium) di-μ5-hydrogenphosphato-penta-μ2-oxo-pentakis[dioxomolybdenum(V)] dihydrate. Acta Crystallographica Section E: Structure Reports Online, 2004, 60, m171-m173.	0.2	1
205	catena-Poly[[aquamanganese(II)]-di-μ-4-pyridylthioacetato-κ6O,Oâ€2:N;N:O,Oâ€2]. Acta Crystallographica Section E: Structure Reports Online, 2004, 60, m169-m170.	0.2	2
206	Bis(1,4-Diazoniabicyclo[2.2.2]octane) octamolybdate(VI) tetrahydrate. Acta Crystallographica Section E: Structure Reports Online, 2004, 60, m359-m361.	0.2	6
207	Tetraaquabis(4-pyridylthioacetato)copper(II). Acta Crystallographica Section E: Structure Reports Online, 2004, 60, m401-m402.	0.2	2
208	Zwitterionic diaqua(1,10-phenanthroline)[3-phosphonopropionato(2–)]zinc(II) dihydrate. Acta Crystallographica Section E: Structure Reports Online, 2004, 60, m941-m942.	0.2	3
209	catena-Poly[[[μ-sulfato-dicopper(I)]-di-μ-4,4â€2-bipyridine-1:1â€2îº2N,Nâ€2;2:2â€2îº2N,Nâ€2] tetrahydrate]. Ac Crystallographica Section E: Structure Reports Online, 2004, 60, m990-m992.	ta 0.2	3
210	catena-Poly[[bis[triaqua[2,5-bis(4-pyridyl)-1,3,4-thiadiazole]cobalt(II)]]-μ4-tetravanadato]. Acta Crystallographica Section E: Structure Reports Online, 2004, 60, m1411-m1413.	0.2	4
211	A Microporous Zinc Phosphonocarboxylate with a Zeolite ABW Framework via the Trialkyl Phosphonocarboxylate Route: In situ Synthesis and Characterization of Na[Zn(O3PC2H4CO2)]·H2O. European Journal of Inorganic Chemistry, 2004, 2004, 544-548.	1.0	37
212	Syntheses, structures and properties of three cluster-based coordination polymers: influence of the metal ions on the ligand coordination mode and crystal chirality. Inorganica Chimica Acta, 2004, 357, 1389-1396.	1.2	19
213	In situ formation of meso-2,2′-oxydisuccinate via intermolecular dehydration coupling ofd,l-malic acid: first coordination polymer of 2,2′-oxydisuccinate involving ether oxygen coordination: [Cd2(meso-odsc)(H2O)]. Dalton Transactions, 2004, , 3437-3439.	1.6	26
214	The three-electron heteropoly blue [P6Mo18O73]11? with a basket-shaped skeletonElectronic supplementary information (ESI) available: UV-vis and EPR spectra, magnetic data, and plot of the arrays of clusters of 1. See http://www.rsc.org/suppdata/cc/b4/b405931j/. Chemical Communications, 2004, , 2046.	2.2	41
215	A novel self-complementary three-dimensional inorganic network organized by H-bond dimers of inorganic chains — Synthesis and crystal structure of (C6H16N2)[Zn(HPO4)2]. Canadian Journal of Chemistry, 2004, 82, 616-621.	0.6	5
216	Linear and Helical Chains in Hydrothermally Synthesized Coordination Polymers [Co(bpdc)(H2O)2] and [Ni(bpdc)(H2O)3]·H2O Involving in situ Ligand Synthesis. European Journal of Inorganic Chemistry, 2003, 2003, 2959-2964.	1.0	54

#	Article	IF	CITATIONS
217	A New Porous 3-D Framework Constructed From Fivefold Parallel Interpenetration of 2-D (6,3) Nets: A Mixed-Valence Copper(I,II) Coordination Polymer [CuI2CuII(4,4′-bpy)2(pydc)2]·4H2O. European Journal of Inorganic Chemistry, 2003, 2003, 413-417.	1.0	67
218	Three-dimensional supramolecular arrays supported by decavanadate clusters: syntheses and crystal structures of (NH4)2[M(dod)(H2O)4]2V10O28·6H2O,. Inorganic Chemistry Communication, 2003, 6, 206-209.	1.8	15
219	Clear Ag–Ag bonds in three silver(I) carboxylate complexes with high cytotoxicity properties. Inorganic Chemistry Communication, 2003, 6, 1113-1116.	1.8	108
220	catena-Poly[[triaquacobalt(II)]-μ-2,3-pyridinedicarboxylato-κ2O2:O3]. Acta Crystallographica Section E: Structure Reports Online, 2003, 59, m1143-m1145.	0.2	1
221	Bis[μ-3-phosphonopropionato(2–)]bis[aqua(1,10-phenanthroline)copper(II)]. Acta Crystallographica Section E: Structure Reports Online, 2003, 59, m1149-m1150.	0.2	3
222	catena-Poly[bis(4-pyridylthioacetato)zinc(II)]. Acta Crystallographica Section E: Structure Reports Online, 2003, 59, m1194-m1195.	0.2	2
223	Title is missing!. Zeitschrift Fur Anorganische Und Allgemeine Chemie, 2003, 629, 1059-1062.	0.6	29
224	DNA-binding property and antitumor activity of bismuth(iii) complex with 1,4,7,10-tetrakis(2-pyridylmethyl)-1,4,7,10-tetraazacyclododecaneElectronic supplementary information (ESI) available: 1H-NMR, ES-MS and CD spectra. See http://www.rsc.org/suppdata/dt/b3/b305290g/. Dalton Transactions, 2003, , 2379.	1.6	22
225	Syntheses, Crystal Structures, and Physical Properties of Dinuclear Copper(I) and Tetranuclear Mixed-Valence Copper(I,II) Complexes with Hydroxylated Bipyridyl-Like Ligands. Chemistry - A European Journal, 2002, 8, 3187.	1.7	191
226	Hydroxylation of N-Heterocycle Ligands Observed in Two Unusual Mixed-Valence Cul/Cull Complexes. Angewandte Chemie - International Edition, 2002, 41, 1029-1031.	7.2	468
227	A novel polycatenated double-layered hybrid organic–inorganic material constructed from [Zn2(tp)(4,4′-bpy)]n2n+ layers and V4O124â^' pillars. Dalton Transactions RSC, 2001, , 770-771.	2.3	88
228	The First Noncluster Vanadium(IV) Coordination Polymers: Solvothermal Syntheses, Crystal Structure, and Ion Exchange. Journal of Solid State Chemistry, 2001, 160, 118-122.	1.4	131